

Correction of X-ray Intensities for Multiple Diffraction: Effects on Atomic Parameters and Charge Density

Bjørn C. Hauback,^A Frode Mo^A and Gunnar Thorkildsen^B

^A Institutt for Fysikk, Universitetet i Trondheim-NTH,
N-7034 Trondheim, Norway.

^B Høgskolesenteret i Rogaland, Ullandhaug,
N-4000 Stavanger, Norway.

Abstract

The standard theory for secondary extinction based on intensity transfer equations has been extended to three-beam diffraction for a finite crystal in the Laue case. The expression for the primary diffracted intensity was used to first order to calculate correction factors for the two-beam integrated power assuming a type I mosaic crystal. The corrections were employed to study the effects of multiple diffraction on structure parameters and deformation density for three different crystals with unit-cell volumes in the range 385–1410 Å³. In these data sets, 5–8% of all reflections with $(\sin\theta/\lambda) \leq 0.7 \text{ \AA}^{-1}$ had relative shifts in integrated power $\Delta P/P > 10\%$. The weak intensities are affected the most, and thus, among the weakest third of the data, 15–21% had relative corrections $>10\%$. The crystallographic R and goodness-of-fit factors were significantly improved after correction of the data for multiple diffraction. Atomic positional and displacement parameters, obtained from the refinements on corrected and uncorrected data respectively, have been compared, as have also pairs of deformation density maps. Rather unexpectedly, all shifts were very small, within 2σ for atomic parameters and within 2.5σ for the deformation densities. This implies that the effects of multiple diffraction are nearly random relative to the structure model and even relative to the deformation density.

1. Introduction

Multiple diffraction (MD) occurs in crystals when more than one reciprocal lattice node (r.l.n.) in addition to the origin lie very close or on the Ewald sphere. The mutual exchange of energy which takes place between the various beams involved may lead to either a diminution (*Aufhellung*), or an enhancement (*Umweganregung*) of the primary diffracted intensities. These effects were first observed by Wagner (1920) and Renninger (1937) respectively. The changes are systematic in the sense that weak reflections in general become enhanced, and strong reflections reduced. Over the last 25 years the importance of the effect of MD on diffracted intensities has been emphasised in a number of articles. Two main strategies have been proposed to reduce the influence of MD: to avoid n -beam interactions, or to identify them and correct the modified intensities.

Santoro and Zocchi (1964) and Coppens (1968) suggested a procedure for elimination of errors in the observed intensities by rotating the crystal about the scattering vector of the primary reflection to positions where no significant intensity perturbations due to MD are observed. However, the geometric

conditions for n -beam diffraction are frequently satisfied, even for a crystal with a relatively small unit cell. The frequency of MD is proportional to V_c/λ^2 , where V_c is the unit cell volume and λ is the wavelength of the incident beam. It may be very difficult or impossible to find a position where multiple scattering effects are negligible, especially for weak primary reflections which are very easily affected by the *Umweg* mechanism. Consequently, it seems necessary to correct for MD in modern, accurate structure work.

Moon and Shull (1964) introduced an approximate treatment of the intensity perturbations due to MD. Tanaka and Saito (1975) have revised and refined this procedure. Other contributions on MD and intensity corrections based on intensity transfer equations are e.g. Zachariasen (1965), Caticha-Ellis (1969), Prager (1971), Parente and Caticha-Ellis (1974), Le Page and Gabe (1979), Soejima *et al.* (1985), Rossmanith (1986), Okazaki *et al.* (1988) and Piltz (1988). Chang (1982) treated the intensity problem for n -beam diffraction in a dynamical formalism. Here we have developed a formalism based on intensity transfer equations within the framework of secondary extinction theories, cf. Becker and Coppens (1974). The results, to first order, are similar to those presented by Tanaka and Saito (1975).

Åsbrink (1970) has compared structure parameters obtained from data sets with and without excess MD due to symmetry. However, the number of interactions and the magnitudes of the intensity corrections were not known. The maximum differences between positional and isotropic thermal parameters were small, less than $3 \cdot 5\sigma$. To our knowledge, a systematic study of the frequency and magnitude of MD, and its effects on refined atomic parameters and deformation density have not been reported before. We present here a theoretical background and experimental results for three different structures. Preliminary results from this work have been given (Hauback and Mo 1987; Mo and Hauback 1987).

2. Theory

(a) Intensity Coupling Equations

We will here describe a formalism for three-beam diffraction in a finite, type I mosaic crystal based on intensity transfer equations (Darwin 1922; Hamilton 1957; Moon and Shull 1964; Zachariasen 1967). These equations can be written in the general form

$$\frac{\partial I_P}{\partial s_P} = -\left(\mu + \sum_{Q \neq P} \sigma_{QP}\right) I_P + \sum_{Q \neq P} \sigma_{PQ} I_Q, \quad (1)$$

where σ_{PQ} is the kinematical diffracting cross section per unit volume and unit intensity for the scattering process $\mathbf{k}_Q \rightarrow \mathbf{k}_P$, with $P, Q \in (O, H, L)$ in the case of three-beam diffraction; \mathbf{k}_O is the wave vector along the incident beam, while \mathbf{k}_H and \mathbf{k}_L are the wave vectors along the primary and secondary diffracted beams respectively; μ is the linear absorption coefficient, and s_P is a coordinate along the unit wave vector $\hat{\mathbf{s}}_P = \mathbf{k}_P/|\mathbf{k}_P|$. The first term on the right side of (1) represents the decrease in intensity of beam I_P due to absorption and energy transfer into all other excited beams I_Q (including the incident beam).

The second term accounts for transfer from all beams I_Q into I_P . Making the transformation

$$I_P = \tilde{I}_P \exp \left\{ - \sum_Q \left(\mu + \sum_{R \neq Q} \sigma_{RQ} \right) s_Q \right\}, \quad (2)$$

we obtain the set of equations

$$\frac{\partial \tilde{I}_P}{\partial s_P} = \sum_{Q \neq P} \sigma_{PQ} \tilde{I}_Q. \quad (3)$$

These equations are identical with the transformed version of Takagi's equations (Thorkildsen 1987).

(b) Boundary-value Green Function for the Intensity Field \tilde{I}_H in Case of Laue Diffraction

The boundary-value Green functions for the intensity fields $\{I_O, I_H, I_L\}$, i.e. the intensities of the beams propagating along \mathbf{k}_O , \mathbf{k}_H and \mathbf{k}_L at the point (s_O, s_H, s_L) due to a point source at the origin, are obtained by applying the boundary conditions

$$I_O(0, s_H, s_L) = \delta(s_H) \delta(s_L), \quad I_H(s_O, 0, s_L) = 0, \quad I_L(s_O, s_H, 0) = 0. \quad (4)$$

The same boundary conditions are valid for the fields $\{\tilde{I}_O, \tilde{I}_H, \tilde{I}_L\}$. Here δ denotes the Dirac δ -function. Due to the similarity with the wave beam formalism, the boundary-value Green functions for the intensity fields can be found by substituting σ_{PQ} for $i\kappa_{PQ}$ in the equations (20a-c) of Thorkildsen (1987). Defining the γ -parameters:

$$\begin{aligned} \gamma_{OH} &= \sigma_{OH} \sigma_{HO}, & \gamma_{OL} &= \sigma_{OL} \sigma_{LO}, & \gamma_{HL} &= \sigma_{HL} \sigma_{LH}, \\ \Gamma_{OHL} &= \sigma_{OL} \sigma_{LH} \sigma_{HO} + \sigma_{OH} \sigma_{HL} \sigma_{LO}, \end{aligned} \quad (5)$$

we have for the intensity field \tilde{I}_H :

$$\begin{aligned} \tilde{I}_H(s_O, s_H, s_L) &= \sigma_{HO} I_0 \{ 2(\gamma_{OH} s_O s_H)^{\frac{1}{2}} \} \delta(s_L) \\ &+ \sum_{m=0}^{\infty} \sum_{n=0}^{\infty} \frac{1}{m! n!} \\ &\times \left(\frac{\sigma_{HO}}{s_L} \frac{I_{2n+m-1} [2 \{ (\gamma_{OL} s_O + \gamma_{HL} s_H) s_L \}^{\frac{1}{2}}]}{\{ (\gamma_{OL} s_O + \gamma_{HL} s_H) s_L \}^{\frac{1}{2}(2n+m-1)}} \right. \\ &+ \left. \sigma_{HL} \sigma_{LO} \frac{I_{2n+m} [2 \{ (\gamma_{OL} s_O + \gamma_{HL} s_H) s_L \}^{\frac{1}{2}}]}{\{ (\gamma_{OL} s_O + \gamma_{HL} s_H) s_L \}^{\frac{1}{2}(2n+m)}} \right) \\ &\times \frac{I_{n+m} \{ 2(\gamma_{OH} s_O s_H)^{\frac{1}{2}} \}}{(\gamma_{OH} s_O s_H)^{\frac{1}{2}(n+m)}} \\ &\times (\Gamma_{OHL} s_O s_H s_L)^m (\gamma_{HL} s_H s_L)^n (\gamma_{OL} s_O s_L)^n, \end{aligned} \quad (6)$$

where the functions I_m are the modified Bessel functions. The field $\tilde{I}_H(s_O, s_H, s_L)$ is not defined for negative values for any of the coordinates. Thus the expression in (6) should be multiplied by $u(s_O)u(s_H)u(s_L)$, where u denotes the unit step function.

(c) *Power and Diffracting Cross Section*

The intensity field $I_H(s_O, s_H, s_L)$ expanded to the lowest order involving the r.l.n. L , thus excluding corrections to the intensity of the primary diffracted beam due to secondary extinction and absorption, becomes

$$I_H(s_O, s_H, s_L) = I_0 \sigma_{HO} \left((1 - \sigma_{LO} s_O - \sigma_{LH} s_H) \delta(s_L) + \frac{\sigma_{HL} \sigma_{LO}}{\sigma_{HO}} \right), \quad (7)$$

where I_0 is the intensity of the incident beam at the entrance surface. For a crystal cut in the shape of a parallelepiped confined by the unit vectors $\hat{\mathbf{s}}_O$, $\hat{\mathbf{s}}_H$ and $\hat{\mathbf{s}}_L$, and with dimensions $l_O \times l_H \times l_L$, integration over the entrance and exit surfaces gives for the power, cf. Moon and Shull (1964):

$$P_H = I_0 \sigma_{HO} v \left\{ 1 - \frac{1}{2} \left(\sigma_{LO} l_O + \sigma_{LH} l_H - \frac{\sigma_{HL} \sigma_{LO}}{\sigma_{HO}} l_L \right) \right\}. \quad (8)$$

To obtain an expression for the integrated power we must evaluate the diffracting cross sections $\{\sigma_{PQ}\}$. Becker and Coppens (1974) have outlined a procedure for calculating σ in the case of two-beam diffraction. Extending to the three-beam case we find for the actual crystal shape:

$$\sigma_{PQ} = |\kappa_{PQ}|^2 I_P \frac{\sin^2(\xi_{PQ}/2)}{(\xi_{PQ}/2)^2}; \quad (9)$$

here

$$|\kappa_{PQ}| = (r_e \lambda / V_c) |F_{P-Q}|, \quad (10)$$

with $1/|\kappa_{PQ}|$ being the extinction length for the actual reflection, r_e is the classical electron radius and $|F_{P-Q}|$ the absolute value of the structure factor involved. The variable ξ_{PQ} is defined through

$$\xi_{PQ} = 2\pi \left\{ K_{PQ} \frac{\sin 2\theta_{PQ}}{\lambda} \epsilon_1 - \alpha_P(\psi) \right\} I_P. \quad (11)$$

Here we have neglected any vertical divergence of the incident beam; ϵ_1 is the angle which measures the horizontal divergence, K_{PQ} is a geometrical factor (Zachariasen 1945), α_P is the excitation error associated with beam \mathbf{k}_P , and ψ is the angle of rotation of the crystal about the scattering vector of the primary r.l.n. Under ordinary diffractometer conditions $\alpha_O = \alpha_H = 0$ and $|K_{HO}| = 1$.

(d) Integrated Power in Type I Mosaic Crystals

Expressions for the correction of intensity data due to multiple diffraction are commonly based on the assumption of a type I mosaic crystal (Zachariasen 1967). In these crystals the width of the intrinsic cross section σ is much less than the width of the mosaic distribution function. This means that

$$\langle I_P K_{PQ} \sin 2\theta_{PQ} \rangle \gg \lambda, \quad (12)$$

$$\langle |K_{PQ}|^2 I_P I_Q \rangle \ll 1, \quad (13)$$

where the second inequality is assumed to assure that dynamical effects, caused by the wave nature of the beams, will be negligible. Equation (12) implies that the diffracting cross section, cf. (9), converges weakly to a Dirac function, i.e.

$$\lim_{I_P \rightarrow \infty} \sigma_{PQ} = \frac{Q_{PQ}}{|K_{PQ}|} \delta \left(\epsilon_1 - \frac{\lambda \alpha_P}{|K_{PQ}| \sin 2\theta_{PQ}} \right), \quad (14)$$

where we have introduced the quantity Q known as the average cross section per unit volume of the crystal, cf. Zachariasen (1945),

$$Q_{PQ} = |K_{PQ}|^2 \frac{\lambda}{\sin 2\theta_{PQ}}. \quad (15)$$

The mosaic distribution function $\tilde{w}_{PQ}^d(\Delta\theta_{PQ})$ is given with respect to the deviation from the Bragg condition, $\Delta\theta_{PQ}$, in the scattering $\mathbf{k}_Q \rightarrow \mathbf{k}_P$. The superscript d denotes the type of distribution function considered. Usually a Gaussian or a Lorentzian distribution function is assumed. Transforming to a representation based on the divergency angle ϵ_1 , we have

$$w_{PQ}^d(\epsilon_1) = |K_{PQ}| \tilde{w}_{PQ}^d(\Delta\theta_{PQ} = |K_{PQ}| \epsilon_1). \quad (16)$$

And the mean diffracting cross section, which is given by a convolution of the intrinsic diffraction function and the mosaic distribution, becomes

$$\bar{\sigma}_{PQ} = \sigma_{PQ} \otimes w_{PQ}^d = Q_{PQ} \tilde{w}_{PQ}^d \left(|K_{PQ}| \epsilon_1 - \frac{\lambda \alpha_P}{\sin 2\theta_{PQ}} \right). \quad (17)$$

Substituting this result for the coupling constant in equation (8), and performing the integration in ϵ_1 , we obtain for the integrated power:

$$P_H = I_0 Q_{HO} \nu \times \left\{ 1 - \frac{1}{2} \left(Q_{LO} I_O W_{LO;HO}^d + Q_{LH} I_H W_{LH;HO}^d - \frac{Q_{HL} Q_{LO}}{Q_{HO}} I_L W_{HL;LO}^d \right) \right\}, \quad (18)$$

where

$$W_{PQ;RS}^d = \int_{-\infty}^{\infty} d\epsilon_1 \tilde{w}_{PQ}^d(\epsilon_1) \tilde{w}_{RS}^d(\epsilon_1). \quad (19)$$

This result is equivalent to equation (9) of Tanaka and Saito (1975). We have, however, used the concept of excitation error, α_L , rather than a delay angle, ζ , to take account of the fact that the two r.l.n. H and L need not be simultaneously on the Ewald sphere.

(e) *Practical Considerations*

To be applicable in the X-ray case polarisation effects must be accounted for in (18) (Zachariassen 1965). As seen from (1), absorption and scattering are coupled in the basic equations. Absorption does not enter the expression for \mathcal{P}_H explicitly, to the order of approximation considered. However the pathlengths l_O, l_H, l_L are calculated as absorption weighted mean pathlengths, cf. Becker and Coppens (1974).

The distribution function \tilde{w}_{PQ}^d is taken to represent the total broadening of a peak profile caused by beam divergence, spectral dispersion, crystal mosaicity and crystal size. In the Gaussian case it is written ($d = \text{Ga}$):

$$\tilde{w}_{PQ}^{\text{Ga}}(\Delta\theta_{PQ}) = \left(\frac{4 \ln 2}{\pi}\right)^{\frac{1}{2}} \frac{1}{x_{PQ}} \exp\left\{-4 \ln 2 \left(\frac{\Delta\theta_{PQ}}{x_{PQ}}\right)^2\right\}, \quad (20)$$

while in the Lorentzian case ($d = \text{Lo}$):

$$\tilde{w}_{PQ}^{\text{Lo}}(\Delta\theta_{PQ}) = \left(\frac{2}{\pi}\right) \frac{1}{x_{PQ}} \frac{1}{1 + (2\Delta\theta_{PQ}/x_{PQ})^2}. \quad (21)$$

Here x_{PQ} is the half-width of the distribution considered. Generally the half-width can be written as $x_{PQ} = x + f(\theta_{PQ})$, where a functional dependence on θ_{PQ} is included to allow for spectral dispersion (Tanaka and Saito 1975; Soejima *et al.* 1985).

More than one secondary reflection are usually close to the Ewald sphere. To first order of approximation it is legitimate to neglect the effect of mutual coupling between the secondary diffracted beams. Thus, the joint effect on the integrated power of the primary diffracted beam is found by summing the contributions from each three-beam case independently. With $I_0 Q_{HO} p_{HO} v$ being the standard kinematical expression for the two-beam integrated power of the primary diffracted beam in the X-ray case [p_{HO} is the polarisation factor $(1 + \cos^2 2\theta_{HO})/2$], the relative change in the integrated power due to three-beam interactions is written:

$$\begin{aligned} \frac{\Delta\mathcal{P}_H}{\mathcal{P}_H} &= \frac{Q_{HO} p_{HO} l_O}{x_{HO}} \\ &\times \sum_L \left\{ -\bar{W}_{LO;HO}^d \left(\frac{Q_{LO}}{Q_{HO}}\right) - \bar{W}_{LH;HO}^d \left(\frac{Q_{LH}}{Q_{HO}}\right) \left(\frac{l_H}{l_O}\right) \right. \\ &\left. + \bar{W}_{HL;LO}^d \left(\frac{Q_{HL}}{Q_{HO}}\right) \left(\frac{Q_{LO}}{Q_{HO}}\right) \left(\frac{l_L}{l_O}\right) \right\}. \quad (22) \end{aligned}$$

The \bar{W} terms represent the product of the appropriate polarisation factor, $x_{HO}/2$ and the W term defined in (19).

The first and second terms in (22) represent a diminution (*Aufhellung*) of the integrated power, the third is an increase (*Umweganregung*). With only one secondary reflection L contributing, and the primary $|F_{HO}|$ small and $|F_{LO}|$ and $|F_{HL}|$ large, *Umweganregung* predominates. *Aufhellung* is favoured when the intensities of the primary and at least one of the secondary and coupling reflections are strong.

The procedure proposed by Tanaka and Saito (1975) can be used to identify the geometrical conditions for MD. All secondary r.l.n. localised within a shell of thickness 2Δ about the Ewald sphere are assumed to satisfy this condition. The thickness of the shell should reflect all the broadening factors of the experiment, however, its exact geometrical shape is not crucial since the strength of an interaction is modified by the damping term $W_{PQ;RS}$, which depends on the actual distance of the corresponding r.l.n. from the Ewald sphere.

Table 1. Crystal data and survey of experimental conditions for 1,2-bis(phenylsulfonyl)ethane modification 1 and 2 (PPDS 1 and 2) and 1,2-bis(methylsulfonyl)ethane (MMDS)

	MMDS	PPDS 1	PPDS 2
Composition	C ₄ H ₁₀ O ₄ S ₂	C ₁₄ H ₁₄ O ₄ S ₂	C ₁₄ H ₁₄ O ₄ S ₂
Space group	<i>P</i> 2 ₁ / <i>c</i>	<i>P</i> 2 ₁ / <i>n</i>	<i>Pna</i> 2 ₁
<i>a</i> (Å)	6·112(5)	8·457(1)	24·249(1)
<i>b</i>	5·907(2)	10·045(1)	11·079(1)
<i>c</i>	10·697(4)	8·965(1)	5·257(1)
β (deg.)	91·53(1)	116·04(2)	90·0
<i>V</i> (Å ³)	386·0(4)	684·3(2)	1412·4(3)
<i>T</i> (K)	86(1)	85(1)	86(1)
λ (Å)	0·71073	0·71073	0·71073
<i>Z</i>	2	2	4
<i>D_x</i> (Mg m ⁻³)	1·6024(17)	1·5063(4)	1·4597(3)
μ (mm ⁻¹) ^A	0·620	0·381	0·370
Size (mm)	~0·61×0·27×0·21	~0·45×0·48×0·48	~0·49×0·22×0·19
Max. (sin θ)/ λ (Å ⁻¹)	1·265	1·265	0·904

^A Mass absorption coefficients taken from 'International Tables for X-ray Crystallography', Vol. IV (1974).

Table 2. Experimental parameters for the MD corrections

	MMDS	PPDS 1	PPDS 2
Δ (Å ⁻¹)	0·002	0·002	0·002
Observed range in half-widths x (deg.)	0·14–0·18	0·14–0·18	0·13–0·17
x used (deg.)	0·15	0·20	0·15
Distribution function	Gaussian	Gaussian	Gaussian

3. Experimental

Table 1 gives crystal data and a survey of the experimental conditions used for the analyses of three different crystals, 1,2-bis(phenylsulfonyl)ethane, (C₁₄H₁₄O₄S₂), the monoclinic PPDS 1, and the orthorhombic modification,

PPDS 2, and 1,2-bis(methylsulfonyl)ethane ($C_4H_{10}O_4S_2$), MMDS. All data sets were collected at 85–6 K without attenuators with Nb-filtered $MoK\alpha$ radiation using the $\omega/2\theta$ scan mode on a Picker FACS-I diffractometer. More complete descriptions of the experiments are given by Thorkildsen (1983) for PPDS 1 and MMDS, and by Hauback and Mo (1990) for PPDS 2. All data sets were corrected for long-term variations, coincidence loss, Lorentz factor, polarisation, scan truncation errors, absorption and extinction. The effects of MD were studied by comparing:

- intensity data uncorrected and corrected for MD,
- the two parent sets of refined structure parameters,
- in two cases, corresponding sections through the deformation density distribution.

Table 2 shows the experimental parameters used in the corrections applying (22). The thickness 2Δ of the shell about the Ewald sphere is probably overestimated as the range of three-beam interactions in these crystals is of the order $0.0005\text{--}0.001 \text{ \AA}^{-1}$. However, the only consequence of retaining values up to 0.002 \AA^{-1} is to include additional multiple-beam cases with negligible correction terms.

The profiles of several three-beam interactions have been studied in detail, and the half-widths x have been evaluated by rotating the crystal about the scattering vector of the primary reflection over the exact three-beam position (ψ -scan). The observed range in x was estimated from several profiles in PPDS 1, PPDS 2 and MMDS. In most cases, the strong secondary and coupling reflections have Bragg angles $\leq 25^\circ$, and line broadening due to wavelength dispersion is very small. The mosaic distribution seemed to be fairly isotropic in the three crystals and, therefore, we have used for each crystal a single isotropic half-width x . The type of distribution function, Gaussian or Lorentzian, was determined according to Helmholtz and Vos (1976).

Absorption weighted pathlengths for the three beams, i.e. l_O, l_H, l_L , were calculated by the analytical method (de Meulenaer and Tompa 1965; Thorkildsen 1983) for PPDS 1 and MMDS. For PPDS 2 average pathlengths, $l_i = 3r/2$, were used,

Table 3. Number of reflections corrected for MD and frequency of large corrections

	MMDS	PPDS 1	PPDS 2	
Range in $s = (\sin\theta)/\lambda$ (\AA^{-1})	<0.75	<0.73	<0.714	>0.714
Total number of refl. corr.	3127	4714	4928	4698
Percent. of all refl. with $\Delta P/P > 5\%^A$	7.6	10.5	9.0	10.9
> 10%	5.9	7.5	5.5	6.2
> 100%	1.6	2.5	1.3	1.1
Percent. of refl. with $w > 0, \Delta P/P > 5\%^A$	5.9	8.3	5.0	0.3
> 10%	4.2	5.4	2.4	0
> 100%	0.7	1.1	0.2	0
F_{\min} , limit in F_0 defining weak refl.	6.7	6.0	10.0	8.7
Percent. of refl. with $F < F_{\min}$	39	34	30	58
Percent. of refl. with $F < F_{\min}$ and $\Delta P/P > 10\%$	14.6	21.0	18.3	10.7

^A $\Delta P/P$ is defined as $(|F|_{\text{corr}}^2 - |F|_{\text{uncorr}}^2)/|F|_{\text{corr}}^2$ where the corrections are due to MD.

where r is the average radius of the crystal. Test calculations showed relatively small changes in the correction factors when average pathlengths were used.

To reduce computing time we required $|F_L|, |F_{H-L}| > F_{\min}$ in the terms for *Aufhellung*, and $|F_{H-L}||F_L|/|F_H| > F_{\min}$ for *Umweganregung* terms. For PPDS 1 and MMDS we used $F_{\min} = 10 \cdot 0$, and for PPDS 2, $F_{\min} = 20 \cdot 0$.

The corrections were calculated with the program M-DIFF (Thorkildsen 1984) on SPERRY 1100 and IBM-AT computers.

4. Results

Table 3 gives the statistics for the MD corrections. For PPDS 1 and MMDS all reflections with $F^2 > \sigma(F^2)$ were given weights $w > 0$. For PPDS 2, the threshold is $2\sigma(F^2)$ and $4\sigma(F^2)$ for data in the ranges $s = (\sin\theta)/\lambda < 0 \cdot 714 \text{ \AA}^{-1}$ and $0 \cdot 714 < s < 0 \cdot 904 \text{ \AA}^{-1}$ respectively. Intensities beyond $s = 0 \cdot 73\text{--}0 \cdot 75 \text{ \AA}^{-1}$ were corrected only in the data for PPDS 2. Even though the fraction of large corrections in this s -range is comparable with that for reflections with $s < 0 \cdot 714 \text{ \AA}^{-1}$, the number of reflections *above threshold* with significant corrections is very small. This is attributable to the very few strong reflection intensities above $s \sim 0 \cdot 70 \text{ \AA}^{-1}$. Therefore, correction of data with $s \leq 0 \cdot 7 \text{ \AA}^{-1}$ seems to be satisfactory.

In the three data sets, 5.5–7.5% of all reflections with $s < 0 \cdot 71\text{--}0 \cdot 75 \text{ \AA}^{-1}$ had $\Delta P/P > 10\%$. As seen from the last rows of Table 3, most of the large corrections involve the weak reflections. Among the weakest third of all intensities, 14.6–21.0% had $\Delta P/P > 10\%$. These fractions are reduced to 7.8–14.8% when only reflections with $w > 0$ are considered. In fact, for the strongest two-thirds of the data, less than 0.4% of the reflections for the three crystals were corrected more than 10%. There were no *Aufhellung* situations with $\Delta P/P > 5\%$.

Table 4. Influence of correction for MD on the averaging of equivalent reflections

The range of reflection considered and definition of weak reflections are given in Table 3

	$R_{\text{int}}^{\text{A}}$ all reflections		R_{int} weak reflections	
	Without corr.	With corr.	Without corr.	With corr.
MMDS, all corr. included	0.018	0.018	0.059	0.051
CORR < 5% ^B neglected		0.017		0.054
PPDS 1, all corr. included	0.017	0.019	0.080	0.062
CORR < 5% ^B neglected		0.016		0.063
PPDS 2, $s < 0 \cdot 714 \text{ \AA}^{-1}$	0.038	0.036	0.211	0.199
$s < 0 \cdot 714 \text{ \AA}^{-1}$	0.104	0.105		

^A The agreement index is $R_{\text{int}} = \Sigma |F_1^2 - F_2^2| / \Sigma F_w^2$, where F_w^2 is the weighted average of F_1^2 and F_2^2 .

^B CORR is the relative correction of $|F|_{\text{uncorr}}^2$.

Two equivalent data sets were measured for each crystal. Results from the merging procedure are given in Table 4. Both data without and with correction for MD were weight-averaged. Corrections for *Aufhellung* tended to reduce the agreement between some strong equivalent reflections, and in addition to the runs including all corrections, merging was also performed neglecting corrections <5% for MMDS and PPDS 1. In the latter case, only *Umweganregung* cases are considered, and the overall R_{int} is slightly improved. As expected,

Table 5. Survey of the refinements

For MMDS and PPDS 1: first row, data not corrected for MD; second row, data corrected for MD and all corrections included; and third row, data corrected for MD and $|\text{CORR}| < 5\%$ neglected. PPDS 2 entries are only given for two first rows

	MMDS	PPDS 1	PPDS 2
$s = (\sin\theta)/\lambda$ (\AA^{-1})	<0.75	<0.75	<0.70
	<0.75	<0.75	<0.70
	<0.75	<0.75	
Scale factor k	10.590(18)	11.874(19)	1.989(3)
	10.602(17)	11.885(18)	1.990(2)
	10.587(17)	11.855(18)	
$R(F) = \Sigma(F_0 - k F_c)/\Sigma F_0 $	0.019	0.025	0.024
	0.017	0.023	0.023
	0.018	0.024	
$R_w(F) = [\Sigma w(F_0 - k F_c)^2/\Sigma wF_0^2]^{\frac{1}{2}}$	0.029	0.036	0.027
	0.027	0.034	0.026
	0.027	0.034	
$\text{GOF} = [\Sigma w(F_0 - k F_c)^2/(\text{NO} - \text{NV})]^{\frac{1}{2}}$ ^A	4.96	7.01	1.97
	4.75	6.64	1.89
	4.78	6.64	
Max. shift/error	0.019	0.013	0.029
	0.001	0.004	0.026
	0.004	0.091	

^A NO is the number of reflections with $w \neq 0$, and NV the number of variables.

R_{int} for the weak reflections is significantly improved in all data sets after corrections for MD.

Some refinement characteristics for the data sets are summarised in Table 5. Both R factors and goodness-of-fit (GOF) are generally improved, in particular the GOF, compared with the least-squares refinements with uncorrected data. The refinements including all correction factors are slightly better than those where corrections $< 5\%$ had been neglected (MMDS and PPDS 1). The shifts in scale factor k are within 2σ .

Table 6. Effect of MD on positional and displacement parameters, and bond lengths and angles

Each entry gives the number of shifts greater than 1σ /largest shift

	Positional parameters	Displacement parameters	Bond lengths	Bond angles
MMDS	1/1.1 σ	0/0.6 σ	1/1.0 σ	1/1.5 σ
PPDS 1	2/1.7 σ	0/0.8 σ	1/1.2 σ	0/0.7 σ
PPDS 2	0/0.9 σ	0/0.9 σ	0/0.6 σ	0/0.5 σ

The influence of MD on refined parameters is shown in Table 6. There are almost no parameter shifts exceeding 1σ . This is rather surprising in view of the large number of significant intensity corrections. The total number of changes $> 1\sigma$ for all parameters is 3, 3 and 0 for MMDS, PPDS 1 and PPDS 2 respectively. It is noteworthy that positional and displacement parameters seem to be equally modified by MD.

Deformation densities are known to be highly sensitive to errors and changes in the data. Therefore, deformation density maps were calculated from corrected and uncorrected data sets for MMDS and PPDS 1, with data below $s = 0.85 \text{ \AA}^{-1}$. Non-hydrogen parameters were taken from refinements with $s > 0.90 \text{ \AA}^{-1}$. All correction coefficients were used. Several sections were calculated through the deformation densities. Fig. 1 shows sections through one of the S-O bonds in the two structures. Figs 1*a* and 1*c* are based on data uncorrected for MD, this correction was included for the calculations of maps (b) and (d). With the standard deviation in the maps estimated at 0.025 e\AA^{-3} away from the nuclear positions, the maximum differences between corrected and uncorrected maps are again unexpectedly small, within 2.5σ for both crystals. The maps excluding *Aufhellung* situations (only corrections $>5\%$ considered) were very similar to those in Fig. 1, and the maximum difference between uncorrected and corrected maps was slightly reduced to 2σ .

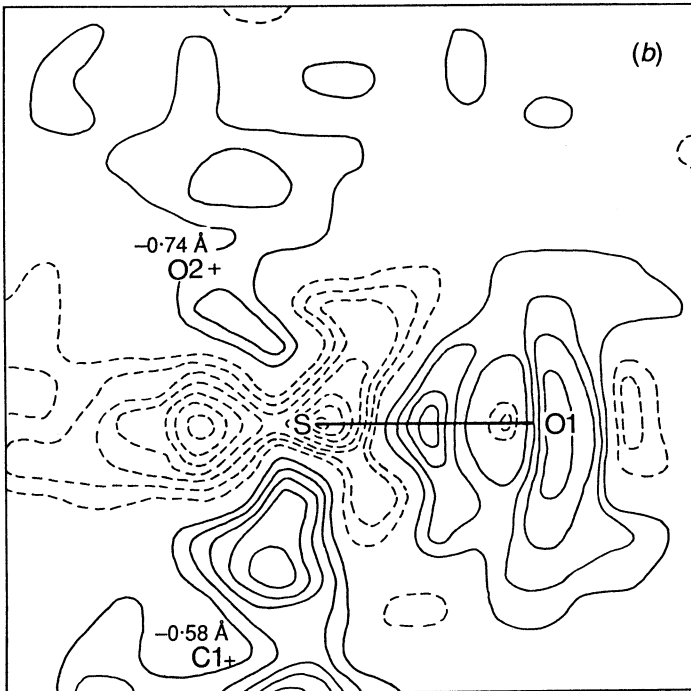
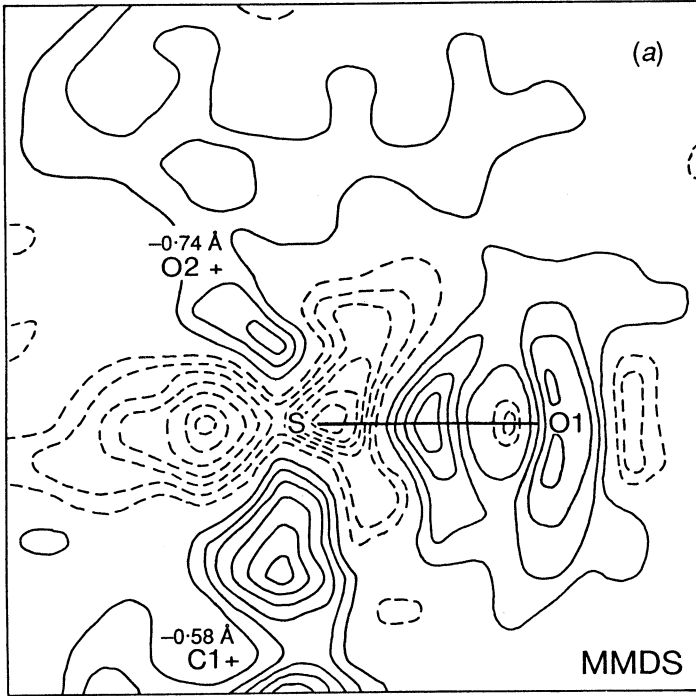
5. Discussion

The ratios of structure factors, the mosaic character and the size and shape of the crystal are important parameters for the magnitude of the intensity shifts. The width of an interaction profile increases and the height decreases with increasing crystal mosaicity. The pathlengths l_p depend on the size and orientation of the crystal, and shorter l_p values in (22) cause reduced intensity perturbations. This effect was also discussed by Moon and Shull (1964) and Åsbrink (1970).

The most critical experimental parameter for calculation of intensity perturbations is the half-width x of the total broadening function. In the present work, we have used a single isotropic value of x for each crystal due to the restricted range of Bragg angles. We obtained good agreement between calculated and observed changes in the integrated power when the corrections were not too large, $\Delta P/P \leq 20\text{--}30\%$. However, large shifts could not be reproduced by (22) with a single value of x . For example, three profiles in PPDS 1 with relative corrections 82–126% had experimental half-widths $x = 0.17\text{--}0.18^\circ$, while x had to be adjusted to 0.13 , 0.36 and 0.58° , respectively, to reproduce the changes in integrated power. For large corrections there is a tendency of the formalism in (22) to overestimate the shifts.

The theory, as developed to lowest order, is based on small extinction and small absorption, which imply $\sigma_{PQ} l_Q \ll 1$ and $\mu l_Q \ll 1$. For the crystals studied, $\sigma_{\max} \sim 0.1 \text{ mm}^{-1}$ while $\mu \sim 0.5 \text{ mm}^{-1}$, and $\mu t \leq 0.2$, where t is the maximum pathlength through the crystal. Thus, the major correction to the approximation involved in (8) is due to absorption. This correction term is

$$\mu \left\{ \left(\frac{l_H^2}{3} + \frac{l_O l_H}{4} \right) \sigma_{LH} + \left(\frac{l_O^2}{3} + \frac{l_O l_H}{4} \right) \sigma_{LO} \right. \\ \left. - \left(\frac{l_L^2}{6} + \frac{l_L l_H}{4} + \frac{l_L l_O}{4} \right) \frac{\sigma_{HL} \sigma_{LO}}{\sigma_{HO}} \right\}.$$



Figs 1a and 1b

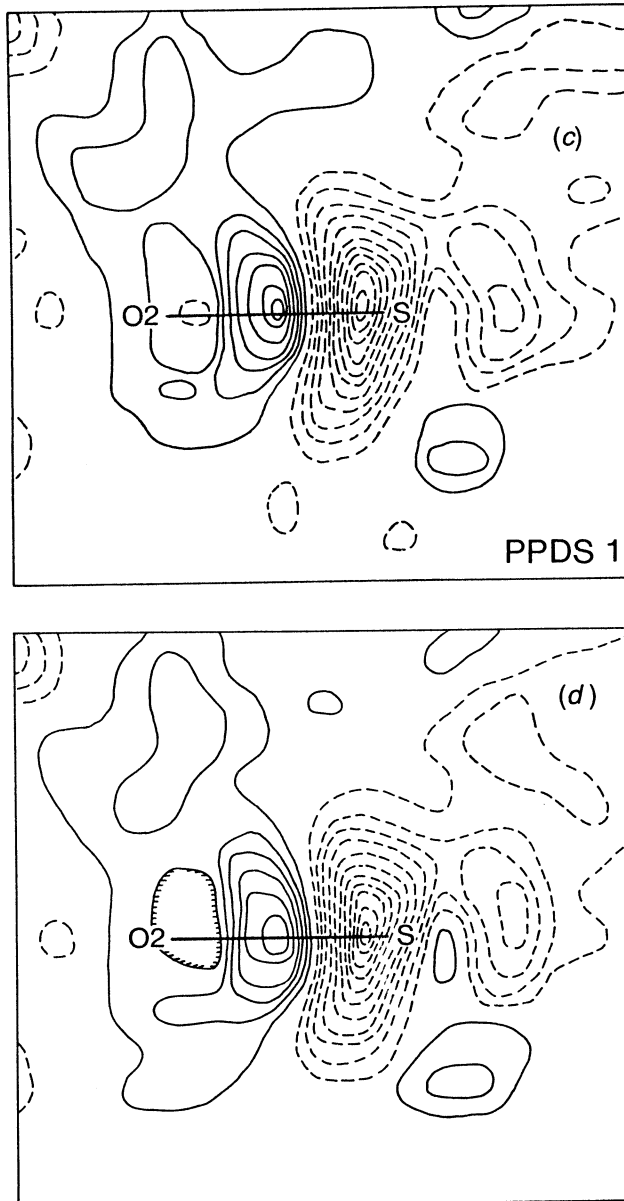


Fig. 1. Deformation density without and with MD. Contours are at $0.05 e\text{\AA}^{-3}$ with negative contours broken, while zero contours are not shown. (a) MMDS: plane through O(1)-S rotated 55° from the normal of O(1)-S-O(2) in a direction towards O(2), without MD correction; (b) as (a), but with MD correction. (c) PPDS 1: plane through O(2)-S perpendicular to O(1)-S-O(2), without MD correction; (d) as (c), but with MD correction.

And consequently, in an *Umweganregung* situation with $l_O \sim l_H \sim l_L \sim l$ we find that the first order change in the power is about 30% too large. Very recently, Piltz (1988) has developed a new set of intensity transfer equations for MD. From a few *Umweganregung* examples, the corrections were significantly improved compared with the application of (1). However, *Aufhellung* situations are treated in the same way by Piltz (1988) and the present authors.

To handle cases with strong interaction between the beams correctly, or in cases where the size of the mosaic grains exceeds the extinction length, dynamical theory, i.e. wave equations, should be used to derive expressions for the intensity perturbations. Values of the power P_H at the exact three-beam point in typical *Umweg* situations, calculated to first order using Takagi's equation (Thorkildsen 1987), show a decrease of about 50% from values obtained with the formalism based on energy transfer equations. Thus, the evaluation of corrections due to three-beam interaction faces much the same problems as the evaluation of corrections for extinction.

The corrections for MD are systematic relative to the distribution of $|F|^2$ in the sense that the predominant effect is a correction of weak intensities for *Umweg* enhancements. Our observations imply that the MD corrections are nearly random relative to the atomic parameters and even to the deformation density, and lead to negligible changes in coordinates and U_{ij} values, and to very small changes in $\delta(\rho)$. There seems to be more noise in the uncorrected maps, and the standard deviations are slightly larger.

To conclude, we observe that MD appears to be a minor source of error in accurate studies of structure and charge density in mosaic crystals. Compared with the problems associated with corrections for extinction and absorption, the effect of MD seems to be of secondary significance.

References

- Åsbrink, S. (1970). *Acta Cryst. A* **26**, 385–90.
 Becker, P. J., and Coppens, P. (1974). *Acta Cryst. A* **30**, 129–47.
 Caticha-Ellis, S. (1969). *Acta Cryst. A* **25**, 666–73.
 Chang, S.-L. (1982). *Acta Cryst. A* **38**, 41–8.
 Coppens, P. (1968). *Acta Cryst. A* **24**, 253–7.
 Darwin, C. G. (1922). *Philos. Mag.* **43**, 800–28.
 de Meulenaer, J., and Tompa, H. (1965). *Acta Cryst.* **19**, 1014–18.
 Hamilton, W. C. (1957). *Acta Cryst.* **10**, 629–34.
 Hauback, B. C., and Mo, F. (1987). *Acta Cryst. Suppl. A* **43**, C224.
 Hauback, B. C., and Mo, F. (1990). *Z. Kristallogr.* (in press).
 Helmholdt, R. B., and Vos, A. (1976). *Acta Cryst. A* **32**, 669.
 'International Tables for X-ray Crystallography' (1974). Vol. IV (Kynoch: Birmingham).
 Le Page, Y., and Gabe, E. J. (1979). *Acta Cryst. A* **35**, 73–8.
 Mo, F., and Hauback, B. C. (1987). Int. Symp. on Accuracy in Structure Factor Measurement, Warburton, Australia, Aug. 1987, Extended Abstr.
 Moon, R. M., and Shull, C. G. (1964). *Acta Cryst.* **17**, 805–12.
 Okazaki, A., Soejima, Y., Machida, M., and Ohe, H. (1988). *Acta Cryst. B* **44**, 568–75.
 Parente, C. B. R., and Caticha-Ellis, S. (1974). *Jpn J. Appl. Phys.* **13**, 1501–5.
 Piltz, R. O. (1988). *Z. Kristallogr.* **185**, 457.
 Prager, P. R. (1971). *Acta Cryst. A* **27**, 563–9.
 Renninger, M. (1937). *Z. Phys.* **106**, 141–76.
 Rossmannith, E. (1986). *Acta Cryst. A* **42**, 344–8.
 Santoro, A., and Zocchi, M. (1964). *Acta Cryst.* **17**, 597–602.

- Soejima, Y., Okazaki, A., and Matsumoto, T. (1985). *Acta Cryst. A* **41**, 128–33.
- Tanaka, K., and Saito, Y. (1975). *Acta Cryst. A* **31**, 841–5.
- Thorkildsen, G. (1983). Doctoral Thesis, Universitetet i Trondheim-NTH.
- Thorkildsen, G. (1984). M-DIFF Working Paper No. 15, Rogaland University, Stavanger.
- Thorkildsen, G. (1987). *Acta Cryst. A* **43**, 361–9.
- Wagner, R. (1920). *Phys. Z.* **21**, 632.
- Zachariasen, W. H. (1945). 'Theory of X-ray Diffraction in Crystals', p. 108 (Wiley: New York).
- Zachariasen, W. H. (1965). *Acta Cryst.* **18**, 705–10.
- Zachariasen, W. H. (1967). *Acta Cryst.* **23**, 558–64.

Manuscript received 4 December 1989, accepted 16 January 1990

